

# On detecting CP violation in a single neutrino oscillation channel at very long baselines

D. C. Latimer<sup>1</sup>, J. Escamilla<sup>2</sup> and D. J. Ernst<sup>2</sup>

<sup>1</sup>*School of Liberal Arts and Sciences, Cumberland University, Lebanon, Tennessee 37087 and*

<sup>2</sup>*Department of Physics and Astronomy, Vanderbilt University, Nashville, Tennessee 37235*

(Dated: August 12, 2021)

We propose a way of detecting CP violation in a single neutrino oscillation channel at very long baselines (on the order of several thousands of kilometers), given precise knowledge of the smallest mass-squared difference. It is shown that CP violation can be characterized by a shift in  $L/E$  of the peak oscillation in the  $\nu_e - \nu_\mu$  appearance channel, both in vacuum and in matter. In fact, matter effects enhance the shift at a fixed energy. We consider the case in which sub-GeV neutrinos are measured with varying baseline and also the case of a fixed baseline. For the varied baseline, accurate knowledge of the absolute neutrino flux would not be necessary; however, neutrinos must be distinguishable from antineutrinos. For the fixed baseline, it is shown that CP violation can be distinguished if the mixing angle  $\theta_{13}$  were known.

PACS numbers: 14.60.Pq

Keywords:

## INTRODUCTION

The vast majority of neutrino oscillation experiments [1, 2, 3, 4, 5, 6, 7] can be understood within a three-neutrino framework [8, 9, 10]. Though oscillation phenomenology is becoming ever more quantitative, there remain unanswered fundamental questions regarding the nature of neutrinos. Oscillation studies will not be able to address some issues; that is, they cannot establish an absolute mass scale of neutrinos or whether neutrinos are their own antiparticles. However, oscillation experiments will be able to shed some light on the level of CP violation in the lepton sector, the relative ordering of the mass eigenstates, and the octant of the  $\theta_{23}$  mixing angle.

In the standard theory of neutrino oscillations, flavor interactions are not diagonal with respect to the mass eigenstates. Instead, flavor states are related to mass eigenstates via a unitary mixing matrix  $U$  which is typically parametrized as in Ref. [11]. This parametrization contains three angles  $\theta_{jk}$ , which indicate the degree of mixing amongst the eigenstates, as well as three phases. The two Majorana phases cannot be probed in oscillation studies so that the Dirac phase  $\delta$  is of sole consequence in this realm. Finally, neutrino oscillations are not sensitive to the absolute mass scale but rather the mass-squared differences,  $\Delta_{jk} = m_j^2 - m_k^2$ . Given three neutrinos, there are two independent mass-squared differences. A current analysis [10] indicates the one- $\sigma$  values for the mixing angles

$$\theta_{12} = 0.59 \pm 0.02, \quad |\theta_{13}| \leq 0.09, \quad \theta_{23} = 0.76 \pm 0.08, \quad (1)$$

and the mass-squared differences

$$\Delta_{21} = 7.9 \pm 0.3 \times 10^{-5} \text{eV}^2, \quad |\Delta_{31}| = 2.6 \pm 0.2 \times 10^{-3} \text{eV}^2. \quad (2)$$

At the moment, there is no knowledge of the Dirac phase and only an upper bound exists on the magnitude of the

mixing angle  $\theta_{13}$ . Additionally, the lack of knowledge regarding the mass hierarchy is reflected in our ignorance of the algebraic sign of  $\Delta_{31}$ .

Future experiments will more precisely determine these parameters as well as address our ignorance of the remaining unanswered questions. Herein, we will focus upon the Dirac CP phase  $\delta$ . CP violation can only be manifest in neutrino oscillations if there are at least three neutrinos with nondegenerate masses and nonzero mixing occurs among all three flavors. Given this, before searching for CP violation, one must first concretely establish that  $\theta_{13}$  is nonzero. The CHOOZ reactor experiment [5] presently establishes the most stringent bound upon this mixing angle; future reactor experiments will achieve much greater sensitivities [12, 13]. Detecting CP violation will be difficult as its effects are modulated by the smallness of  $\theta_{13}$ . As an added complication, for relatively long baselines through the earth, interactions with matter can result in differences between neutrino and antineutrino oscillations, even in the absence of intrinsic CP violation. This “fake” signal is not a consequence of a nontrivial CP phase but is due to the fact that the earth is made of matter (and not antimatter). Finally, ignorance of the mass hierarchy can create difficulties when trying to extract intrinsic CP violation from such channels.

To ascertain the level of CP violation in the lepton sector, one might compare neutrino and antineutrino appearance channels over the same baseline. This underpins many experimental proposals; see Ref. [14] and the references contained therein. These experiments require long baselines; however, they are still in a regime in which the mass-squared dominance approximation is valid to first order in the ratio  $\Delta_{21}/\Delta_{31}$ . Should  $\theta_{13}$  not be too small, one could also, in principle, see the effects of CP violation within a single neutrino oscillation channel. In

fact, an index for characterizing the level of CP violation ascertained from a single-channel oscillation was developed in Ref. [15], as an analog to the usual asymmetry index used when CP conjugate channels are operable [16]. Herein, we will consider the effect of CP violation upon a single oscillation channel. We begin by examining a neutrino appearance channel in vacuum and then consider neutrinos which traverse a constant density mantle; the region of interest will require very long baselines in which terms involving  $\Delta_{21}$  cannot be linearized.

## VACUUM OSCILLATION

An understanding of the case of vacuum oscillations will guide our efforts. We will use the standard parametrization of the PMNS mixing matrix  $U$  [11]. The probability that an  $\alpha$ -flavor neutrino of energy  $E$  will be detected as a  $\beta$ -flavor neutrino at a baseline  $L$  is

$$\begin{aligned} \mathcal{P}_{\alpha\beta}(L/E) = & \delta_{\alpha\beta} - 4 \sum_{\substack{j>k \\ j,k=1}}^3 \Re(C_{jk}^{\alpha\beta}) \sin^2(\varphi_{jk}) \\ & + 2 \sum_{\substack{j>k \\ j,k=1}}^3 \Im(C_{jk}^{\alpha\beta}) \sin(2\varphi_{jk}), \end{aligned} \quad (3)$$

with  $C_{jk}^{\alpha\beta} := U_{\alpha j} U_{\alpha k}^* U_{\beta k} U_{\beta j}^*$  and  $\varphi_{jk} = 1.27 \Delta_{jk} L/E$  where the neutrino mass-squared differences  $\Delta_{jk} = m_j^2 - m_k^2$  are in  $\text{eV}^2$  and the ratio  $L/E$  is in units of  $\text{km}/\text{GeV}$ . Recalling that the CP phase changes sign when considering antineutrinos, we see that the first sum in the oscillation probability consists of CP even terms whereas the last sum consists of CP odd terms provided  $\alpha \neq \beta$ . In appearance channels  $\alpha \neq \beta$ , the coefficients of each term in the sum are proportional to the Jarlskog invariant  $J$  [17]

$$\Im(C_{jk}^{\alpha\beta}) = J \sum_{\gamma l} \epsilon_{\alpha\beta\gamma} \epsilon_{jkl}. \quad (4)$$

With the standard parametrization one has

$$J = s_{12} c_{12} s_{13} c_{13}^2 s_{23} c_{23} s_{\delta}, \quad (5)$$

where  $s_{jk} = \sin \theta_{jk}$  and so on. Given that the CP odd terms are modulated by  $s_{13}$ , the mixing angle  $\theta_{13}$  must be appreciable to detect CP violation. If one were able to maximize terms linear in  $s_{13}$  then CP violating effects would be as large as possible. Note that to most easily work with linear in  $\theta_{13}$  terms, we allow for negative  $\theta_{13}$  mixing angles as proposed in [18]. In Refs. [19, 20], we noted that such terms will be largest whenever the oscillation probability achieves a local maximum due to the smaller mass-squared difference  $\Delta_{21}$ ; as such, this is a fruitful region in which to explore the effects of CP violation.

What then is the effect of the CP phase on a single appearance channel? For the CP even terms, the phase makes an appearance in the form of  $\cos \delta$ . Its size can modify the amplitude of the oscillation probability to order  $\delta^2$ . Of more interest are the CP odd terms. Sizable CP violation results in a phase shift of oscillation phases  $\varphi_{jk}$ ; that is, for a given set of mixing angles and mass-squared differences, the peak oscillation probabilities will occur at a different value of  $L/E$ . If the phase shift is significant, then perhaps a broadband measurement around a local maximum would measure such a shift; or alternatively, a varying baseline experiment could be used to determine the position of the maximum. This presumes sufficient previous knowledge of the mass-squared differences, and this shift in the local maximum cannot independently resolve both  $\theta_{13}$  and  $s_{\delta}$ .

As the two mass-squared differences  $\Delta_{21} \approx 8 \times 10^{-5} \text{ eV}^2$  and  $\Delta_{32} \approx 2 \times 10^{-3} \text{ eV}^2$  are well separated, regions exist where oscillations can be approximated by a quasi-two-neutrino scenario. We first examine the region in which oscillations due to the  $\Delta_{21}$  mass-squared difference is negligible. To first order, the remaining mass-squared differences are degenerate,  $\Delta_{31} \approx \Delta_{32}$ . This near equality causes the CP odd terms, given by,

$$\begin{aligned} \sum_{\substack{j>k \\ j,k=1}}^3 \Im(C_{jk}^{\alpha\beta}) \sin(2\varphi_{jk}) & \approx J[\sin(2\varphi_{31}) - \sin(2\varphi_{32})] \\ & \approx 0. \end{aligned} \quad (6)$$

to be zero to first order.

A better region to explore is where the  $\Delta_{21}$  driven oscillations are appreciable and the oscillations due to the larger mass-squared differences are unresolvable. In this region, we may approximate

$$\langle \sin^2(\varphi_{3j}) \rangle \approx \frac{1}{2}, \quad \langle \sin(2\varphi_{3j}) \rangle \approx 0, \quad (7)$$

for  $j = 1, 2$ . Here, oscillations  $\nu_e \leftrightarrow \nu_{\mu}$  are the dominant mode, so we will focus upon the appearance channel  $\mathcal{P}_{e\mu}$ . To first order, this probability is

$$\mathcal{P}_{e\mu} \approx -2\Re(C_{31}^{e\mu} + C_{32}^{e\mu}) - 4\Re(C_{21}^{e\mu}) \sin^2(\varphi_{21}) - 2J \sin(2\varphi_{21}). \quad (8)$$

The constant term due to the unresolvable higher frequency oscillations can be written as

$$-2\Re(C_{31}^{e\mu} + C_{32}^{e\mu}) = 2s_{13}^2 c_{13}^2 s_{23}^2; \quad (9)$$

this term is small as the mixing between mass eigenstates 1 and 3 is small. The coefficient of the CP even term can be written as

$$-4\Re(C_{21}^{e\mu}) = 4[s_{12}^2 c_{12}^2 c_{13}^2 (c_{23}^2 - s_{13}^2 s_{23}^2) + (c_{12}^2 - s_{12}^2) K], \quad (10)$$

where we define  $K := s_{12} c_{12} s_{13} c_{13}^2 s_{23} c_{23} c_{\delta}$ .

We wish to characterize the effect of CP violation in a single oscillation channel  $\mathcal{P}_{e\mu}$ . As such we will compare the consequences of maximal CP violation with no CP violation. First, let us determine the form of the oscillation probability whenever CP is conserved. We adopt the convention in Ref. [18, 21] in which we restrict the CP phase  $\delta \in [0, \pi)$  and allow negative mixing angle  $\theta_{13} \in [-\pi/2, \pi/2]$ . For no CP violation  $\delta = 0$ , one has  $J = 0$  and  $K = K_{\max} = s_{12}c_{12}s_{13}c_{13}^2s_{23}c_{23}$ . Given this, with CP symmetry conserved, the  $\nu_e - \nu_\mu$  oscillation probability is

$$\mathcal{P}_{e\mu} \approx A + B_{CPC} \sin^2(\varphi_{21}) \quad (11)$$

with  $A = 2s_{13}^2c_{13}^2s_{23}^2$  and  $B_{CPC} = 4[s_{12}^2c_{12}^2c_{13}^2(c_{23}^2 - s_{23}^2) + (c_{12}^2 - s_{12}^2)K_{\max}]$ . Using the best fit mixing angles in Eq. (1) for  $\theta_{12}$  and  $\theta_{23}$  as well as the 1- $\sigma$  bound for  $\theta_{13}$ , one has  $A = 0.008$  and  $B_{CPC} = 0.47$ . As  $\theta_{13}$  is small, the contribution of the  $K_{\max}$  term to  $B_{CPC}$  is on the order of 6%. The first oscillation maximum in this region occurs whenever  $\varphi_{21} = \pi/2$ . Using the best fit mass-squared difference in Eq. (2), one finds this maximum at a baseline to energy ratio of  $L/E = 1.57 \times 10^4$  km/GeV. The maximum value of the oscillation probability is 0.48.

When CP violation is maximal  $\delta = \pi/2$ , one has  $J = J_{\max} = s_{12}c_{12}s_{13}c_{13}^2s_{23}c_{23}$  and  $K = 0$ . Given this, with maximal CP violation, the oscillation probability is

$$\mathcal{P}_{e\mu} \approx A + B \sin^2(\varphi_{21}) + C \sin(2\varphi_{21}) \quad (12)$$

with  $A$  as above,  $B = 4s_{12}^2c_{12}^2c_{13}^2(c_{23}^2 - s_{23}^2)$ , and  $C = -2J_{\max}$ . With some rearrangement, one may combine the two terms which are dependent upon the oscillation phase to achieve

$$\mathcal{P}_{e\mu} \approx A' + B' \sin^2(\varphi_{21} + \phi) \quad (13)$$

with the new terms

$$A' = A + \frac{1}{2}(B - \sqrt{B^2 + 4C^2}), \quad B' = \sqrt{B^2 + 4C^2}, \quad (14)$$

and phase shift

$$\sin(2\phi) = \frac{2C}{B'}. \quad (15)$$

Comparing with no CP violation, we note two differences: there is a slight shift in the maximum value of  $\mathcal{P}_{e\mu}$  and a shift in the value of  $L/E$  at which this maximum occurs. From the mixing angles in Eq. (1), one notes  $4C^2 \ll B^2$  so that to a good approximation  $A' \approx A - C^2/B$ . Additionally, there is an adjustment in the depth of the oscillation probability; one has  $B' \approx B + 2C^2/B$ . Comparing the maximum value of the oscillation probability for the CP conserving (CPC) and maximally violating (CPV) cases, we find

$$(\mathcal{P}_{e\mu}^{CPC})_{\max} - (\mathcal{P}_{e\mu}^{CPV})_{\max} \approx 4 \cos(2\theta_{12})K_{\max} - \frac{C^2}{B}; \quad (16)$$

this difference represents a small shift in the maximum value of around 6%.

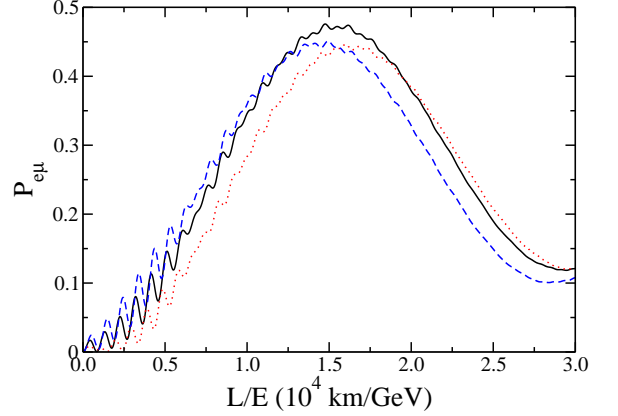


FIG. 1: [color online] The curves represent  $\nu_e - \nu_\mu$  oscillation probabilities in vacuum at a long baseline for the parameters indicated in the text. A detector resolution has been included in the curve. The (black) solid curve is the case in which CP is conserved. The (red) dotted curve is the case in which CP is maximally violated with  $\theta_{13} = 0.09$ . The (blue) dashed curve is the case in which CP is maximally violated with  $\theta_{13} = -0.09$ .

Perhaps more interesting is the value of  $L/E$  for which these maxima occur. This is found from the relative phase shift  $\phi$  between the two sine functions. Using the small angle approximation, one has

$$\phi \approx \frac{C}{B} \left( 1 - \frac{2C^2}{B^2} \right). \quad (17)$$

Keeping the first order terms in the mixing angle  $\theta_{13}$  and approximating maximal mixing for  $\theta_{23}$ , one has

$$\phi \approx -\frac{\theta_{13}}{\sin(2\theta_{12})}. \quad (18)$$

As expected, the shift in phase is proportional to the mixing angle  $\theta_{13}$ . Using the usual mixing angles from Eq. (1), we find a phase shift of  $\phi = -5^\circ$ . We note that should  $\theta_{13} = -0.09$  (a negative angle), then the phase shift would be  $\phi = +5^\circ$ .

In Fig. 1, we see that this phase shift results in a shift in the position of the oscillation peak. We compare the  $\nu_e - \nu_\mu$  oscillation probabilities at very long baselines for the CPC case and the two CPV cases. We use the mixing angles and mass-squared differences from Eqs. (1–2) and mimic detector resolution so that the rapid oscillations due to the larger mass-squared difference are present in the “wiggles” but are damped out. The peak probability for the CPC curve (solid line) occurs at  $L/E = \pi/(2.54\Delta_{21}) = 1.67 \times 10^4$  km/GeV as expected. Relative to this, the CPV peak probability (dotted line) with positive  $\theta_{13}$  leads by an  $L/E$  of  $0.18 \times 10^4$  km/GeV, or lags (dashed line) by an equal amount for

negative  $\theta_{13}$ . The height of the peak and the width of the peak decrease by a small amount for the CPV cases.

In analyzing such data, it would be key to know the small mass-squared difference,  $\Delta_{21}$ , with a high degree of precision. Additionally, we have taken for  $\theta_{13}$  its  $1\text{-}\sigma$  bound; if this mixing angle were smaller, the relative shifts in the two probability curves would be proportionally smaller and more difficult to detect. Clearly, to make measurements around  $L/E \sim 10^4$  km/GeV one would need a *very* long baseline through the earth's mantle. For neutrinos of energy 0.5 GeV, for instance, this would occur at a baseline of 5000 km. Matter effects then become quite significant so we next include them in the analysis.

## OSCILLATION IN MATTER

Neutrinos which travel through sufficiently dense matter undergo coherent forward scattering. Neutral current interactions produce no change in oscillation as all flavors interact equally. Charged current interactions, however, result in an effective potential for the electron flavor only [22]. In the flavor basis, the neutrino evolution equation in matter becomes

$$i\partial_t \nu_f = \left[ \frac{1}{2E} U \mathcal{M} U^\dagger + \mathcal{V} \right] \nu_f \quad (19)$$

where the mass-squared matrix is  $\mathcal{M} = \text{diag}(0, \Delta_{21}, \Delta_{31})$  and the operator  $\mathcal{V}$  operates on the electron flavor with a magnitude  $V = \sqrt{2} G_F N_e$ , with  $G_F$  the Fermi coupling constant and  $N_e$  the electron number density. For simplicity we shall assume matter of constant density. This will avoid the possibility of parametric resonances [23] which could obscure the features we wish to highlight. For a mantle density of  $4.0 \text{ g/cm}^3$  [24, 25], the matter potential is about  $V \sim 1.5 \times 10^{-13} \text{ eV}$ . For anti-neutrinos, one needs to change the algebraic sign of this potential. For anti-neutrinos, the MSW effect suppresses the oscillations and widens the peak so we will confine ourselves to the superior neutrino oscillation channel below.

For producing results pictured in the graphs, we exactly solve Eq. (19). To best understand the origin of the effects seen, it is instructive to examine approximate analytical expressions for the oscillation probabilities. A constant density mantle is a relatively good approximation; however, it limits our baseline to less than 5000 km [26]. This, in turn, places a limit upon the neutrino energy if we are to reach the peak of the  $\Delta_{21}$  oscillations. As a result, we will only consider neutrino energies below 1 GeV.

For such neutrinos traversing the earth, matter affects are most easily understood using the approximations developed in Ref. [27]; see also Ref. [20]. With a constant density, one may diagonalize Eq. (19) to achieve effective mixing angles in matter  $\theta_{jk}^m$  as well as modified mass-squared differences  $\Delta_{jk}^m$ . For the current scenario, the

mass-squared difference of most interest effectively becomes

$$\Delta_{21}^m \approx \Delta_{21} \sqrt{\cos^2 2\theta_{12} (1 - E/E_R)^2 + \sin^2 2\theta_{12}}, \quad (20)$$

where the resonance energy is

$$E_R = \frac{\Delta_{21} \cos 2\theta_{12}}{2V c_{13}^2}. \quad (21)$$

The remaining mass-squared differences are modified as well; however, the limit of incoherent oscillations used above for vacuum oscillations, Eq. (7), is still valid here. The mixing angle most severely affected by the matter is  $\theta_{12}$ ; effectively, one has

$$\sin 2\theta_{12}^m \approx \frac{\sin 2\theta_{12}}{\sqrt{\cos^2 2\theta_{12} (1 - E/E_R)^2 + \sin^2 2\theta_{12}}}. \quad (22)$$

The correction also results in a modified mixing angle

$$\theta_{13}^m \approx \theta_{13} + \frac{\sin 2\theta_{13} E V}{\Delta_{31}}. \quad (23)$$

Finally, the remaining mixing angle  $\theta_{23}$  is unaffected by matter. We note that the only point at which a linear power of the mass-squared difference  $\Delta_{31}$  enters is in the modification of  $\theta_{13}$ . This correction for matter effects is quite small so that our results will be independent of the (unknown) neutrino hierarchy at the level of a 10% adjustment to the (already small)  $\theta_{13}^m$ . We will assume normal hierarchy so that  $\Delta_{31} > 0$ .

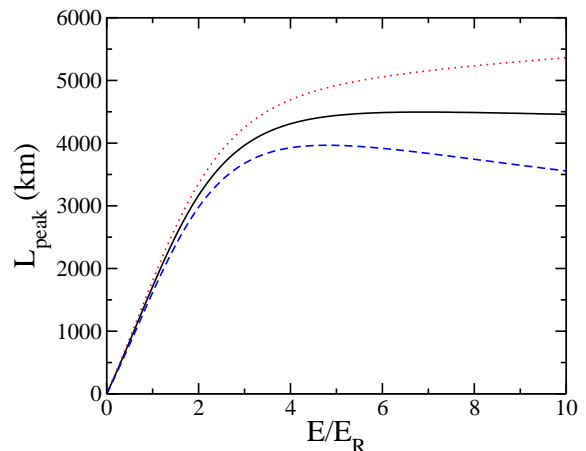


FIG. 2: [color online] Baseline for the first peak of the  $\nu_e\text{-}\nu_\mu$  appearance probability driven by the effective mass-squared difference  $\Delta_{21}^m$ . The resonant energy in the mantle is  $E_R = 0.10 \text{ GeV}$  for the assumed neutrino parameters. The (black) solid curve is the case in which CP is conserved. The (red) dotted curve is the case in which CP is maximally violated with  $\theta_{13} = 0.09$ . The (blue) dashed curve is the case in which CP is maximally violated with  $\theta_{13} = -0.09$ .

In this constant density mantle, the form of the oscillation probabilities developed in Eqs. (11–13) is unchanged; one merely needs to replace all quantities with

their effective value in matter. From those expressions, we explore the consequences upon the very long baseline appearance channel. Given matter effects, the oscillation phase  $\varphi_{21}$  now has additional energy dependence, thereby modifying the baselines needed to measure the peak of the  $\mathcal{P}_{e\mu}^{CPC}$  curve. In Fig. 2, we plot, as a function of energy, the baseline needed to measure the first peak,  $L_{\text{peak}} = \pi E / (2.54 \Delta_{21}^m)$ . In the plot, we express the energy in terms of the resonance energy; for the mixing angles and mass-squared differences assumed herein, the resonance energy in the mantle is around 0.10 GeV. For oscillations in vacuum, the curve would be linear; however, in matter, the baseline  $L_{\text{peak}}$  decreases with energy, relative to vacuum oscillations, as the matter term begins to dominate the kinetic term in  $\Delta_{21}^m$ . If CP were maximally violated, then the baseline for the peak is shifted according to the phase shift  $\phi^m$  which also carries an energy dependence by virtue of the modified mixing angles. As with the vacuum case, a positive (negative) mixing angle  $\theta_{13}$  will result in a longer (shorter) baseline relative to the CPC conserved case; this is demonstrated by the dotted (dashed) curve in Fig. 2.

The fact that the separation between CPC and CPV peak oscillation probabilities increases with energy is attributable to the energy dependence of the phase shift in matter  $\phi^m$ . Improving on the  $5^\circ$  phase shift from the vacuum case would aid in resolving the size of the Dirac phase. We recall the definition of the phase shift, Eq. (15), and substitute the appropriate mixing angles in matter. The change in the mixing angles is most profound for  $\theta_{12}$ ; in fact, we see from Eq. (22) that this mixing angle vanishes as  $1/E$  for large energies. This is seen in Fig. 3.

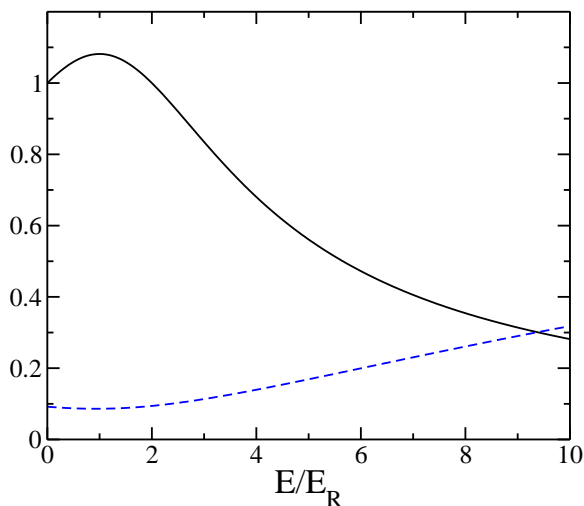


FIG. 3: [color online] The (black) solid line is the ratio  $\sin 2\theta_{12}^m / \sin 2\theta_{12}$ . The (blue) dashed line is the phase shift (expressed in radians) in matter,  $\phi^m$ , with  $\theta_{13} = -0.09$ .

As a result, the term  $B^m$  vanishes for large energies resulting in the limit  $\phi^m \rightarrow \pi/4$ . This represents the max-

imum phase shift between a CPC and maximally CPV peak. The dashed curve in Fig. 3 shows how  $\phi^m$  increases for the energy range under consideration here. (Note that we use  $\theta_{13} = -0.09$  so that we may plot a positive phase shift on the same graph.) The  $\theta_{12}$  factor contributes a term linear in energy which also combines with the correction to  $\theta_{13}$  resulting in a small quadratic contribution. At  $E = 0.5$  GeV, the phase shift is about  $10^\circ$ ; for  $E = 1$  GeV, the shift has risen to  $18^\circ$ , thus enhancing the sensitivity to CP violation.

In addition to the phase shift, the height of the peak value for the oscillation probability will be modified by matter effects. Recalling the coefficients  $B_{CPC}$  and  $B'$ , we note that the amplitudes of the oscillations are dominated by  $\sin^2 2\theta_{12}^m$  in the energy region of interest. As such, the peak value for the appearance channel will decrease with energy. With increased energies, matter effects enhance the phase shift between the CPC and CPV cases; however, at the same time, the value of the oscillation maxima decreases, requiring a more intense beam or larger detector to maintain equal sensitivity.

## VARYING BASELINE

Given the background of the approximate analytical framework above, we shall now show exact numerical results which demonstrate the features derived above. We continue with a constant density mantle and use the same oscillation parameters as above, but now we solve the propagation equation, Eq. (19), sans approximation. Our interest is in the position of the peak oscillation in an appearance channel. Since locating a peak can be done without knowing the absolute normalization of the beam (typically a large systematic error in an experiment), this approach holds a distinct advantage. To locate a peak, a spread in  $L/E$  is required. This can be effected by varying the baseline for a fixed energy or measuring a broadband neutrino beam at a fixed baseline.

We first consider a varying baseline for a narrowband neutrino beam. Sub-GeV atmospheric neutrinos would be the most likely source for such an experiment. Unfortunately, a water Cherenkov counter such as Super-Kamiokande [3] does not have the precision needed to determine the path length of lower energy neutrinos given the large scattering angle between the detected lepton and the incident neutrino. Additionally, such detectors do not have the ability to resolve neutrino from anti-neutrino which is here needed to achieve a clean signal. Future detectors, such as a magnetized iron calorimeter [14], might have sufficient ability to detect the sub-GeV atmospheric neutrinos while identifying whether they are particle or antiparticle. Despite the fact that the absolute flux of atmospheric neutrinos is only known to within 15%, the proposed method of detecting CP violation is not sensitive to this as it is the shape of the oscillation

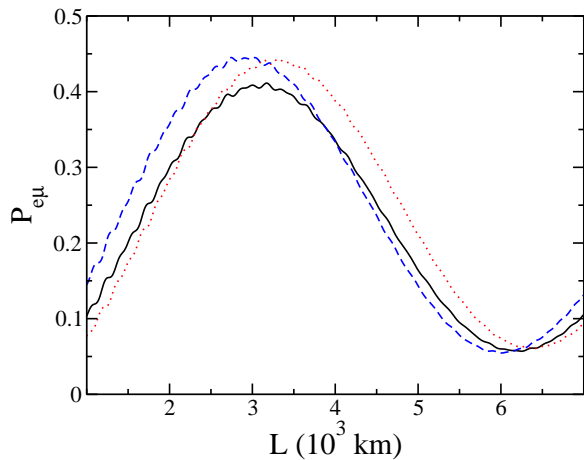


FIG. 4: [color online] The curves represent  $\nu_e$ - $\nu_\mu$  oscillation probabilities through a constant density mantle at a varying baselines for neutrinos with a narrow energy band of  $E_\nu = 0.2$  GeV. A detector resolution has been included in the curves. CP is conserved for the (black) solid curves. CP is maximally violated with  $\theta_{13} = 0.09$  for the (red) dotted curves. CP is maximally violated with  $\theta_{13} = -0.09$  for the (blue) dashed curves.

probability curve which is the determining factor. Introducing a finite detector resolution, we plot the appearance probability in Figs. 4–6 for three neutrino energies. We include the CPC case and the two CPV cases with  $\theta_{13} = \pm 0.09$ . Notice that the vertical and horizontal

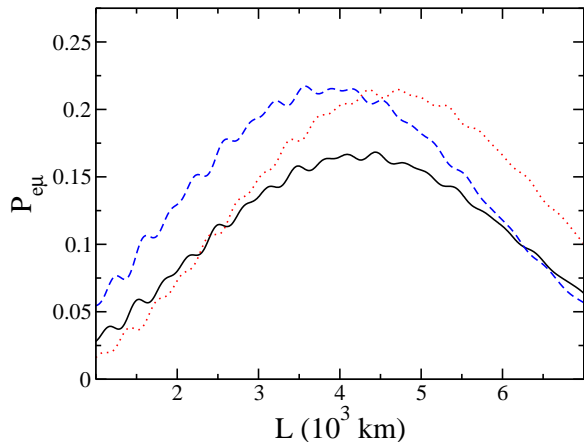


FIG. 5: [color online] The same as Fig. 4 except  $E_\nu = 0.4$  GeV.

axes differ between the three curves. Upon examination, we note that the peaks of all curves are roughly located by the approximate baseline indicated in Fig. 2; the separation increases with energy. Note that the height of the peaks decreases with increasing energy, caused by the energy dependence of  $\sin^2(2\theta_{12}^m)$ ; this decrease in amplitude effectively broadens the peaks. For energies above 0.5 GeV, the peak of the CPC probability remains relatively near 4500 km while the peaks of the CPV curves move

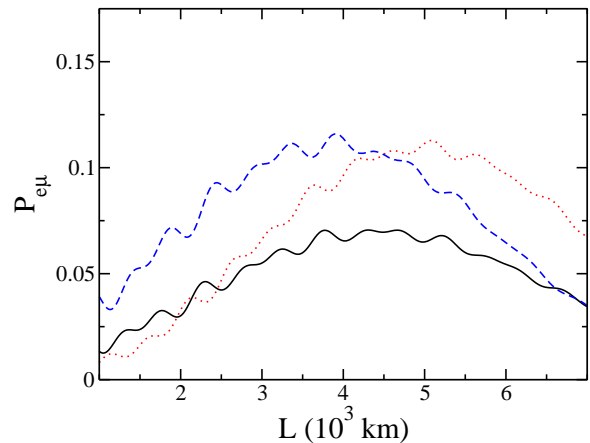


FIG. 6: [color online] The same as Fig. 4 except  $E_\nu = 0.6$  GeV.

farther away from this point. For instance, at 0.6 GeV, the peak of the CPV curve with  $\theta_{13} = -0.09$  is 3900 km, and the peak for the CPV curve with  $\theta_{13} = 0.09$  is around 5100 km. We note too that there is a relatively significant difference in the peak value of oscillation between the CPC and maximally CPV cases. How these features might be seen in an atmospheric neutrino experiment is left for future work.

## FIXED BASELINE

Fixed very long baseline experiments have been previously considered in the literature as a means to uncover CP violation, the value of  $\theta_{13}$ , and discerning the mass hierarchy [14]. Typically, such experiments have baseline and neutrino energies that still permit a dominant mass-squared difference approximation to first or second order. As noted previously, we presently consider the other extreme in which the oscillations due to the larger mass-squared differences are unresolvable. As a source of neutrinos, we envision an accelerator beam stop. Using an additional detector near the source allows one to have a better estimate on the expected flux at a far detector. Also, one can potentially control whether the beam is running in a neutrino or antineutrino mode making it inconsequential as to whether the detector can distinguish the two. This fact would allow one to make use of existing technologies, such as water Cherenkov detectors. In terms of our proposal, present technology would need to be extended to give lower energies in order to reach the needed values of  $L/E$ .

To consider a fixed baseline detector, we will simulate a broad band neutrino beam with energies ranging from 0.1 to 0.4 GeV with a flat spectrum. As we now are dealing with a range of energies, the effective mixing angles and mass-squared differences are no longer constant despite the constant density approximation. The phase



shift between the CPC and CPV cases will manifest itself differently than in the fixed energy case. In Fig. 2, we plot the baseline for which the oscillation phase  $\varphi_{21}^m$  achieves the value  $\pi/2$  in the constant density mantle, which simplified the analysis for fixed energy. There is no such simplification for a fixed baseline.

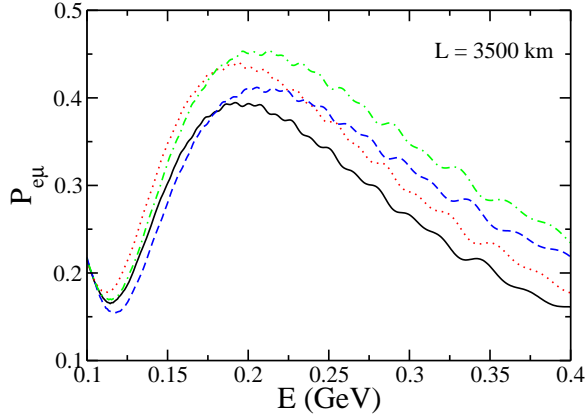


FIG. 7: [color online] The curves represent  $\nu_e$ - $\nu_\mu$  oscillation probabilities through a constant density mantle at a fixed baseline of 3500 km. CP is conserved for the (black) solid curve with  $\theta_{13} = 0.09$  and the (green) dot-dashed curve with  $\theta_{13} = -0.09$ . CP is maximally violated for the (red) dotted curve with  $\theta_{13} = 0.09$  and the (blue) dashed curve with  $\theta_{13} = -0.09$ .

The maximum value of the appearance channel not only depends upon the oscillatory phase  $\varphi_{21}^m$  but also upon the energy dependent amplitude of the oscillation. Recall, the energy dependence of the amplitude is dominated by  $\sin^2(2\theta_{12}^m)$  which sharply decreases for energies greater than twice the resonant energy. On the other hand, for energies below twice the resonant energy, oscillation can be enhanced relative to the vacuum. This factor must be included in determining the ideal baseline. Incorporating these two factors, we can determine the effect of baseline upon the detected neutrino spectrum. As an example, we examine a baseline around 4500 km. From Fig. 2, the oscillatory phases for the maximal CPV case with  $\theta_{13} = 0.09$  and the CPC case achieve the value of  $\pi/2$  at 0.35 GeV and 0.62 GeV, respectively. However, as the CPC peak occurs at a higher energy its amplitude will be suppressed relative to the CPV case so that the two  $\mathcal{P}_{e\mu}$  curves could be readily distinguished. Turning to the CPV case with  $\theta_{13} = -0.09$ , we note that at this baseline the oscillatory phase  $\varphi_{21}$  is greater than  $\pi/2$  for all energies under consideration. As a result, the oscillation probability is further suppressed relative to the other two cases. In Figs. 7–9, we plot  $\mathcal{P}_{e\mu}$  for three very long baselines. A horizontal shift (in  $L/E$ ) of the location of the oscillation peaks is difficult to discern; however, there is a considerable relative vertical shift in the height of the curves. As this vertical shift is of import, we also plot the case in which CP is conserved but with negative mix-

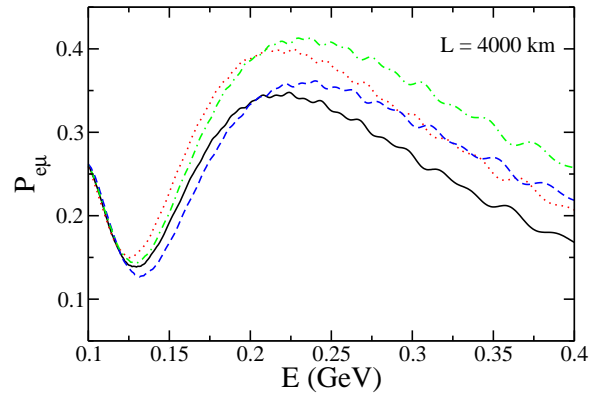


FIG. 8: [color online] The same as Fig. 7 except with a baseline of 4000 km.

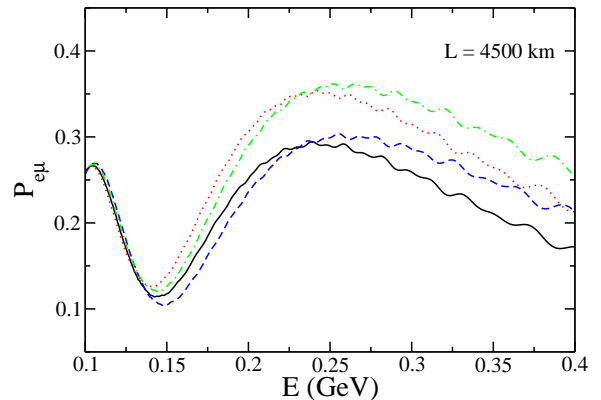


FIG. 9: [color online] The same as Fig. 7 except with a baseline of 4500 km.

ing angle  $\theta_{13} = -0.09$ . In Ref. [19], it was shown that a negative mixing angle will shift the oscillation probability vertically at these baselines and energies. Taken as a whole, there is no real signature amongst these curves which can characterize both the level of CP violation and the sign of  $\theta_{13}$ . However, if one assumed knowledge of  $\theta_{13}$ , then there is a clear separation between the CPC and CPV curves. As an example, we consider the CPC and CPV curves for both having  $\theta_{13} = 0.09$ , the solid (black) curve and the dotted (red) curve at the baseline of 4000 km. The percent difference between the peaks of these curves is 14%. A similar relationship holds for the curves for  $\theta_{13} = -0.09$ , the dashed (blue) and the dash-dot (green) curves. Thus, should  $\theta_{13}$  become known and not be too small, this becomes a possible experiment for searching for CP violation.

## CONCLUSION

We examined a means of detecting CP violation in a single neutrino oscillation channel. Such methods would require a non-zero value of  $\theta_{13}$  as well as a precise knowl-

edge of the small mass-squared difference. The CP phase was found to have the most profound impact for very long baselines at low energies, i.e., near the first peak of the oscillatory region of the smaller mass-squared difference. By examining a single oscillation channel, one avoids the possibility of a fake signal of CP violation attributable to matter effects. Additionally, for the energies and baselines under consideration, mass hierarchy does not enter at a significant level. It was shown that CP violation can be characterized by a shift (in  $L/E$ ) of the peak of the appearance channel relative to CP conservation, both in vacuum and with MSW matter effects. In fact, matter effects enhance the shift at a fixed energy, and the effect is most pronounced for a varying baseline experiment rather than a fixed very long baseline. The best source for examining this effect is in atmospheric data, as fixing  $E$  and varying  $L$  is not so practical. For this accurate knowledge of the absolute neutrino flux is not necessary; however, neutrinos must be distinguishable from antineutrinos. Unfortunately, the matter-induced energy dependence of the parameters obscures the shift (in  $L/E$ ) of the peak at fixed baselines. However, the height of such peaks exhibits significant dependence on  $\delta$  so that the level of CP violation could be resolved if  $\theta_{13}$  were known. Finally, the proposed measurements likely could not resolve the  $\theta_{13}$ - $\delta$  degeneracy.

D. C. L. thanks the Institute for Nuclear Theory at the University of Washington for its hospitality during this work. This work was supported, in part, by U S Department of Energy Grant DE-FG02-96ER40975.

- 
- [1] B. T. Cleveland *et al.*, *Astrophys. J.* **496**, 505 (1998); J. N. Abdurashitov *et al.*, *Phys. Rev. C* **60**, 055801 (1999); J. Exp. Theor. Phys. **95**, 181 (2002); W. Hampel *et al.*, *Phys. Lett.* **B447**, 127 (1999); M. Altmann *et al.*, *Phys. Lett.* **B490**, 16 (2000); Q. R. Ahmad *et al.*, *Phys. Rev. Lett.* **87**, 071301 (2001); *Phys. Rev. Lett.* **89**, 011301 (2002); S. N. Ahmed, *Phys. Rev. Lett.* **92**, 181301 (2004).
  - [2] K. Eguchi *et al.*, *Phys. Rev. Lett.* **90**, 021802 (2003); T. Araki *et al.*, *Phys. Rev. Lett.* **94**, 081801 (2005).
  - [3] Y. Fukuda *et al.*, *Phys. Lett.* **B335**, 237 (1994); **B433**, 9 (1998); **B436**, 33 (1998); *Phys. Rev. Lett.* **81**, 1562 (1998); *Phys. Lett.* **B436**, 33 (1998); *Phys. Rev. Lett.* **82**, 2644 (1999); **86**, 5651 (2001); Y. Ashie *et al.*, *Phys. Rev. Lett.* **93**, 101801 (2004); *Phys. Rev. D* **71**, 112003 (2005).
  - [4] M. H. Ahn *et al.*, *Phys. Rev. Lett.* **90**, 041801 (2003); *Phys. Rev. Lett.* **93**, 051801 (2004); E. Aliu *et al.*, *Phys. Rev. Lett.* **94**, 081802 (2005).
  - [5] M. Apollonio *et al.*, *Phys. Lett.* **B420**, 397 (1998); **B466**, 415 (1999); *Eur. Phys. J. C* **27**, 331 (2003).
  - [6] D. G. Michael *et al.*, *Phys. Rev. Lett.* **97**, 191801 (2006).
  - [7] A. A. Aguilar-Arevalo, *Phys. Rev. Lett.* **98**, 231801 (2007).
  - [8] V. Barger, D. Marfatia and K. Whisnant, *Int. J. Mod. Phys. E* **12**, 569 (2003).
  - [9] G. L. Fogli, E. Lisi, A. Marrone and A. Palazzo, *Prog. Part. Nucl. Phys.* **57**, 742 (2006).
  - [10] M. C. Gonzalez-Garcia and M. Maltoni, arXiv:0704.1800 [hep-ph].
  - [11] W.M. Yao *et al.*, *J. Phys. G* **33**, 1 (2006).
  - [12] F. Ardellier *et al.*, arXiv:hep-ex/0606025.
  - [13] X. Guo *et al.*, arXiv:hep-ex/0701029.
  - [14] V. Barger *et al.*, "Report of the US long baseline neutrino experiment study", arXiv:0705.4396 [hep-ph]; V. Barger, P. Huber, D. Marfatia, and W. Winter, *Phys. Rev. D* **76**, 031301 (2007).
  - [15] K. Kimura, A. Takamura and T. Yoshikawa, *Phys. Lett.* **B642**, 372; **B640**, 32 (2006).
  - [16] C. Jarlskog, *Phys. Rev. Lett.* **55**, 1039 (1985).
  - [17] C. Jarlskog, *Phys. Lett.* **B609**, 323 (2005).
  - [18] D. C. Latimer and D. J. Ernst, *Phys. Rev. D* **71**, 017301 (2005).
  - [19] D. C. Latimer and D. J. Ernst, *Phys. Rev. C* **71**, 062501(R) (2005).
  - [20] D. C. Latimer and D. J. Ernst, *Phys. Rev. C* **72**, 045502 (2005).
  - [21] J. Gluza and M. Zralek, *Phys. Lett.* **B517**, 158 (2001).
  - [22] L. Wolfenstein, *Phys. Rev. D* **17**, 2369 (1978); S. P. Mikheev and A. Y. Smirnov, *Sov. J. Nucl. Phys.* **42**, 913 (1985) [*Yad. Fiz.* **42**, 1441 (1985)].
  - [23] E. K. Akhmedov, A. Dighe, P. Lipari and A. Y. Smirnov, *Nucl. Phys.* **B542**, 3 (1999).
  - [24] A. M. Dziewonski and D. L. Anderson, *Phys. Earth Planet. Inter.* **25**, 297 (1981).
  - [25] E. Lisi and D. Montanino, *Phys. Rev. D* **56**, 1792 (1997).
  - [26] V. Barger, D. Marfatia, and K. Whisnant, *Phys. Rev. D* **65**, 073023 (2002).
  - [27] O. L. G. Peres and A. Yu. Smirnov, *Nucl. Phys.* **B680**, 479 (2004).